



Published in final edited form as:

*J Stroke Cerebrovasc Dis.* 2020 September ; 29(9): 105078. doi:10.1016/j.jstrokecerebrovasdis.2020.105078.

## The Role of Microstructural Integrity of Major Language Pathways in Narrative Speech in the First Year after Stroke

Zafer Keser, MD<sup>1,2,\*</sup>, Erin L. Meier, PhD,CCC-SLP<sup>2</sup>, Melissa D. Stockbridge, PhD,MSc<sup>2</sup>, Argye E. Hillis, MD,MA.<sup>2</sup>

<sup>1</sup>Department of Neurology, The University of Texas Health Science Center, Houston TX

<sup>2</sup>Department of Neurology, Johns Hopkins University School of Medicine, Baltimore, MD

### Abstract

**Background and Purpose**—Left hemisphere stroke often results in a variety of language deficits due to varying patterns of damage to language networks. The Cookie Theft picture description task, a classic, quick bedside assessment, has been shown to quantify narrative speech reliably. In this study, we utilized diffusion tensor imaging (DTI) to assess language network white matter tract correlates of lexical-semantic and syntactic impairments longitudinally.

**Methods**—Twenty-eight patients with mild to severe language impairments after left hemispheric lobar and/or subcortical ischemic stroke underwent the Cookie Theft picture description test and DTI up to three different time points: within the first three months, six months and twelve months after stroke. Dorsal and ventral stream language pathways were segmented to obtain DTI integrity metrics of both hemispheres. Multivariable regression models and partial correlation analyses adjusted for age, education, and lesion load were conducted to evaluate the temporal DTI profile of the white matter microstructural integrity of the language tracts as neural correlates of narrative speech within the first year after stroke.

**Results**—Among all the major language white matter pathways, the integrity of the left arcuate (AF), inferior fronto-occipital, and inferior longitudinal fasciculi (ILF) were related to picture description performance. After FDR correction, left ILF fractional anisotropy correlated with syntactic cohesiveness ( $r=0.85, p=0.00087$ ) within the first three months after stroke, whereas at one year post-stroke, the strongest correlations were found between lexical-semantic performance and left AF radial diffusivity ( $r=-0.71, p=0.00065$ ).

**Conclusion**—Our study provides a temporal profile of associations between the integrity of the main language pathways and lexical semantics and syntactic impairments in left hemispheric strokes.

### Keywords

Stroke; Aphasia; Narrative Speech; Diffusion Tensor Imaging (DTI)

---

\*Corresponding Author: Zafer Keser, MD, Department of Neurology, The University of Texas Health Science Center, Houston, TX, Johns Hopkins University School of Medicine, Baltimore, MD, Mailing Address: 6431 Fannin Street Suite 7.044, Houston, TX 77030. zafer.keser@uth.tmc.edu, zkeser1@jhmi.edu, Phone: +1-409-434-8189.

**Declaration of Interest:** None.

## Introduction

Stroke is one of the most common acquired neurological disorders and the leading cause of disability, and one-third of stroke survivors suffer from varying degrees of aphasia.<sup>1–2</sup> Post-stroke aphasia is a complex disorder that arises from heterogeneous pathologies in large convoluted networks in the brain;<sup>3–5</sup> thus, revealing its natural progression and recovery patterns remains difficult.<sup>6</sup> However, understanding post-stroke aphasia recovery patterns is equally crucial to individualize treatment intensity and strategies, as many diverse language deficits may persist.<sup>1</sup> In order to characterize the neural correlates of the post-stroke speech impairment, the majority of previous work mostly focused on lesion and symptom mapping, but this technique has significant limitations, such as inability to capture the downstream effects of the lesions and potential discordance between the location of lesions and dysfunction.<sup>7</sup>

Diffusion tensor imaging (DTI) is an advanced magnetic resonance imaging (MRI) technique that can be utilized to assess the microstructural integrity of white matter pathways. Extraction of diffusion scalars from atlas-segmented white matter tracts is a widely used technique to assess the microstructural integrity of the tracts.<sup>8–11</sup> While there are more cross-sectional DTI studies,<sup>10, 12–16</sup> there is scarce literature on longitudinal DTI studies in aphasia. A subset of the longitudinal studies showed changes in WM integrity as a function of therapy in chronic aphasia<sup>17–20</sup> or that higher pre-treatment WM integrity of left temporal tracts is associated with better treatment outcomes.<sup>11,21</sup> For natural recovery mechanisms, imaging values at the acute time point such as asymmetry in the integrity of AF,<sup>22</sup> the absence of left AF,<sup>23</sup> and left hemisphere global lesion load<sup>24</sup> predicted the global aphasia measures six months after stroke. Our study evaluates the temporal DTI profile of the white matter microstructural integrity of the ventral and dorsal stream pathways longitudinally in a subset of patients for whom multiple imaging sessions were available in order to provide neural correlates of narrative speech components within the first year after a left hemispheric stroke.

The Cookie Theft single-picture description,<sup>25</sup> part of the National Institute of Health Stroke Scale and Boston Diagnostic Aphasia Examination, is a brief bedside assessment that was previously shown to quantify two main components of the narrative speech; lexical-semantic content<sup>26–28</sup> and syntactic cohesion<sup>29</sup> in post-stroke aphasia. Content is quantified through the analysis of a speaker's included *content units* (CU). CUs refer to the most frequently identified subjects and actions elicited by the stimulus in a comprehensive description by healthy controls. CUs can be either explicit or implicit. In contrast, cohesion refers to the use of language to refer to content across sentences, such that a sentence's meaning can only be fully understood in relation to other sentences. This skill relies on the appropriate use of parts of speech, such as referents (e.g., pronouns and determiners) as well as noun restatements (e.g., mother, mommy, lady), to convey clearly and unambiguously that a reference to something outside of the sentence has occurred (e.g., "Joe is in the park. *He* is playing lacrosse.").

Language impairment after stroke is a complex phenomenon, and most previous studies investigated the individual subcomponents of the disorder.<sup>3–5,8</sup> Thus, in this study, we

investigated temporal changes in the microstructural integrity of the main white matter pathways within the language network and their associations to narrative speech over the first year following left hemisphere stroke.

## Methods

The datasets analyzed during the current study are available from the corresponding author on reasonable request. Twenty-eight native English-speaking patients (see table 1 for demographics) with clinically diagnosed mild to severe aphasia after left hemispheric lobar and subcortical ischemic stroke were enrolled in the study. Concurrent imaging and behavioral data were collected at acute/subacute (<3months after stroke), early chronic (4–7 months after stroke), and late chronic (11–13 months after stroke) time points. Ten out of twenty-eight subjects had at least two data points at acute/subacute and early or late chronic time points, and these subjects' data were utilized in the additional longitudinal analyses. The study subjects only received standard of care speech therapy during the study. Ethics approval was obtained from the local institutional review board of Johns Hopkins University School of Medicine, and written informed consent was obtained from all the patients.

## Behavioral Measures

Cookie Theft spoken picture descriptions were audio-recorded and transcribed by trained research personnel. They were then scored for CU and analyzed for cohesion by experienced research speech-language pathologists. CUs are words or phrases, or their synonyms, mentioned by healthy controls in describing this picture.<sup>26</sup> Number of CUs was chosen as a dependent variable in our analysis because it differentiates healthy controls and aphasic patients and provides a reliable measure of aphasia severity,<sup>26</sup> strongly correlates with lesion volume<sup>28</sup> and with scores on longer language assessments (e.g., Boston Naming Test).<sup>30</sup>

Cohesion provides a complementary measure of narrative speech related to syntactic production. Cohesive ties were assessed following the protocol outlined in Liles and Coelho.<sup>31</sup> Ties that are unambiguous are said to be “complete.” The systematic and convergent method of cohesion analysis presented in Liles and Coelho's work<sup>31</sup> is considered a highly reliable adaptation of the original cohesion analysis described in Halliday and Hasan's study.<sup>32</sup> A subset of the samples used in this analysis was more comprehensively described for cohesion strategies and success in our group's study.<sup>29</sup> In order to reduce the number of dependent variables resulting from typical cohesion analysis, the present work focused on a single measure of completeness (proportion of complete ties to total ties) for only two strategies for establishing linguistic cohesion: personal referents (personal pronouns) and lexical cohesion. Performance appeared bimodal for both strategies, with scores clustering at 0 and 1. Based on this observation, values were further reduced to a categorical distinction: 0–0.49 reflecting poor completeness in cohesion and 0.50–1 reflecting relatively intact completeness in cohesion.

## MRI acquisition and preprocessing

Whole-brain MRI data including high-resolution T1weighted, T2weighted, Fluid Attenuated Inversion Recovery (FLAIR), and Diffusion-weighted imaging (DWI) were acquired on a

Philips 3T scanner by using a SENSE receive head coil. 3D sagittal acquired T1-weighted magnetization prepared rapid acquisition with gradient echo (MPRAGE) had a spatial resolution of  $1\text{ mm} \times 1\text{ mm} \times 1\text{ mm}$ , and field of view (FOV) was  $256 \times 256$ . T2 weighted spin-echo images were acquired axially with a slice thickness of 2 mm with no gaps, FOV= $212 \times 212$ , TR/TE:4171/12, and FLAIR with 5 mm slice thickness and FOV:512/512. DWI data were acquired axially with no gaps and a total of 32 diffusion orientations (one of them was b0). TR/TE:7013/71, FOV= $212 \times 212$  mm, the b-value/slice thickness/in-plane resolution was 700s  $\text{mm}^2/2.2\text{mm}/0.82\text{mm}$ . DWI data files were converted into nifti format in dcm2nii ([nitrc.org/plugins/mwiki/index.php/dcm2nii:MainPage](http://nitrc.org/plugins/mwiki/index.php/dcm2nii:MainPage)) or MRIconvert ([icni.uoregon.edu/downloads/mriconvert](http://icni.uoregon.edu/downloads/mriconvert)). Nifti files were then uploaded to DSIstudio ([dsistudio.labsolver.org](http://dsistudio.labsolver.org)). The source images were inspected for significant movement artifacts, and the eddy motion correction was performed. Diffusion-weighted images were then resampled at 1 mm isotropic. The b-table was checked by an automatic quality control routine to ensure its accuracy.<sup>33</sup>

### Lesion Load Segmentation

Lesion load included white matter (WM) hyperintensities and infarct volumes and were quantified manually in MRICron software ([nitrc.org/projects/mricron](http://nitrc.org/projects/mricron)) by an experienced neurologist in lesion segmentation with using high-resolution T2-weighted and FLAIR and T1 weighted images. For the normalization of the volumes of WM hyperintensities and infarcts, the total intracranial volume (ICV) was estimated by summing all segmented WM, GM, and CSF from each subject by using DWI-b0 and T1 weighted maps. The lesion load was calculated as the percentage of total lesion volume to ICV (lesion load= lesion volume/ICV  $\times$  100). Once the lesion load was obtained, it was used as an independent variable in the regression models. Thus, the lesion load was only used in the statistical analyses but not automatically masked out from the tracts in the native imaging space.

### Atlas Based Tract Segmentation

DSI Studio was used to calculate the tensor-based on an algorithm described elsewhere<sup>34</sup> to obtain fractional anisotropy (FA;  $\mu \pm \sigma$ ), and radial diffusivities (RD;  $\times 10^{-3}\text{ mm}^2\text{ s}^{-1}$ ). FA and RD scalar maps were used as they reflect the white matter integrity accurately in various conditions.<sup>8,9</sup> The atlas-based segmentation function in DSI studio was then conducted to obtain atlas-based segmentation of the right and left AF, SLF, frontal aslant tract, inferior fronto-occipital fasciculus (IFOF), inferior longitudinal fasciculus (ILF), uncinate fasciculus (UF) (Figures 1) by warping Human Connectome Project white matter atlas ([www.humanconnectomeproject.org/](http://www.humanconnectomeproject.org/)) into individual subject space. Tract parcellations were then edited with neuroanatomy guidance (i.e., moving the volume of interest in 3D space, smoothing, thresholding)<sup>35</sup> on a slice by slice basis on DTI maps with an FA threshold of 0.15<sup>8</sup>, that also eliminated the significantly injured tissues.

### Statistical Analyses

We conducted a recursive feature selection with 10-fold cross-validation in the entire dataset by fusing all the different time points of all the tract values and both CU and cohesion scores, to remove redundant predictors.<sup>36-37</sup> This method is a backward elimination method that computes the importance for each predictor.<sup>24</sup> The least important predictors were

removed, and the model was re-built multiple times until the significant predictors were obtained for CU and cohesion scores ( $p < 0.05$ ). Linear and logistic regression analyses were also performed separately for each time point (acute/subacute, early chronic, late chronic). A separate regression model was created for longitudinal analyses that explored the prediction of the behavioral outcomes at early or late chronic time points (whichever is available) by using tract variables at acute/subacute time point. The multivariable linear model, including CUs as the dependent variable and tract measures, age, education, and lesion load as independent variables, was used. Next, a multivariable logistical regression model was calculated for the lexical and personal cohesion performance category, including tract measures, age, education, lesion load. A p-value of less than 0.05 considered significant. We then conducted partial Pearson correlations for the variables in the linear regression models and partial Spearman correlations for the variables included in the logistic regression models. After obtaining p-values, the false discovery rate (FDR) analysis of 5% was also conducted for multiple comparison analyses. Area under the curve (AUC) analyses were used to assess the prediction model accuracy in both linear and logistic regression models, and odds ratio was calculated for the logistic regression model (for FA, the increment was selected as 0.01 and for RD, 0.02 arbitrarily as a reference point). R statistical package was used for the statistical analyses.

## Results

Recursive feature selection analysis showed that the FA and RD of left AF, IFOF, and ILF were found to be the best predictors of clinical outcomes and were used in further analyses. AF, IFOF, ILF, and CU variables were descriptively illustrated with individual points for each person, as different people had values for each time point in Figure 2. Concurrent imaging and behavioral measures at each time point were used. Significant results are also highlighted in Table 2 and Figure 3. The lesion load in the cohort was  $1.24 \pm 0.79$ .

### Acute/Subacute Timepoints

None of the tract values at acute/subacute time points showed a significant relation with acute/subacute CU. However, in the longitudinal model, left AF RD at baseline (acute/subacute) predicted later (early or late chronic-whichever is available) CU ( $r = -0.64$ ,  $p = 0.025$ ), but this correlation became insignificant after FDR correction. Acute/subacute personal pronoun cohesiveness was significantly correlated with acute/subacute left AF FA ( $r = 0.66$ ,  $p = 0.028$ ) and left ILF FA ( $r = 0.85$ ,  $p = 0.00087$ ) (Figure 3). Only the relation between acute/subacute ILF FA and acute/subacute personal pronoun cohesiveness remained significant after FDR correction.

### Early Chronic Timepoints

Only left AF FA ( $r = 0.45$ ,  $p = 0.01$ ) and left ILF RD ( $r = -0.47$ ,  $p = 0.01$ ) significantly correlated with CU in the early chronic time point. These associations became insignificant after FDR correction.

## Late Chronic Timepoints

In this time point, left AF FA and RD showed significant association with CU ( $r=0.60$ ,  $p=0.005$ , and  $r=-0.71$ ,  $p=0.00065$ , respectively) (Figure 3). Left IFOF FA and RD showed a similar significant trend ( $r=0.49$ ,  $p=0.01$  and  $r=0.57$ ,  $p=0.004$  respectively) as well as left ILF FA ( $r=0.43$ ,  $p=0.02$ ) and left ILF RD ( $r=-0.60$ ,  $p=0.003$ ). For this time point, left AF FA and RD showed significant association with personal pronouns cohesiveness ( $r=0.57$ ,  $p=0.02$ , and  $r=-0.59$ ,  $p=0.007$ , respectively). Left Only left AF RD remained significant after FDR correction.

## Discussion

In this study, we explored the role of the major ventral and dorsal language pathways and their homologous pathways in lexical-semantic retrieval and syntactic cohesion in a cohort of individuals with left hemispheric ischemic stroke. After controlling for potential confounding variables and correcting for multiple analyses, we showed that left AF was the best correlate of lexical-semantic retrieval, especially a year after the injury. The integrity of left ILF in the first three months was the best correlate of syntactic cohesion. Additionally, microstructural integrity of left AF predicted recovery in lexical-semantic retrieval, but this prediction did not survive FDR correction, likely due to a small sample size. Despite a limited number of subjects with longitudinal data in our cohort, this study provides preliminary evidence in temporal changes and longitudinal predictive roles of the main language pathways in specific speech and language functions, while most previous DTI studies have reported a single cross-sectional relationship.<sup>10-13,15,38,39</sup>

“The left AF has also been shown to be related to lexical-semantic tasks such as picture naming, semantic verbal fluency, sentence comprehension.<sup>10,14</sup> The left middle temporal gyrus was previously found to be critical in the lexical storage,<sup>40</sup> whereas angular gyri in visual lexical retrieval.<sup>41</sup> The left inferior frontal gyrus, although classically known to be the main hub for speech production, plays a crucial role in semantic retrieval.<sup>42</sup> Our findings align well with previous findings<sup>10-15,43,44</sup> as the left AF connecting the left inferior frontal gyrus to the superior and middle temporal gyri as well as angular, and supramarginal gyri (Figure 1A) was found to be the best correlate of production of CU, which demands lexical-semantic retrieval. However, this relation was only significant in the late chronic time point. Integrity of left AF was more related to semantic retrieval at the late chronic time point, consistent with recent models of the main roles of the dorsal stream. Our data indicate that AF is likely to be related to recovery of lexical-semantic retrieval.

Left ILF was shown to be related to semantic interference in comprehension, semantic paraphasias, and picture-word matching.<sup>45,46</sup> Consistent with previous studies showing the importance of superior temporal gyri<sup>47</sup> and left anterior inferior temporal lobe<sup>48</sup> and temporoparietal junction in syntactic processing, the left ILF connecting anterior and inferior temporal regions to posterior superior temporal gyrus, temporoparietal junction and lateral occipital regions (Figure 1C) was found to be the best correlate of syntactic cohesiveness within first three months after the injury. Thus, the left ILF in the ventral stream appears to have a role in syntactic processing (cohesiveness) at the acute timepoint.



At this point, the reason for these temporal brain structure and function relations remains unclear, and further studies are needed to explore further and validate our findings.

Right hemispheric pathways showed no association with our measures of lexical-semantic retrieval and syntactical cohesion. As previously shown, the integrity of the right hemisphere homologous language pathways plays a negative role in picture naming<sup>8</sup> and a positive role in fluency-based tasks.<sup>18,49</sup> In another study, the volume of one subsegment of right AF, the long segment, positively predicted global aphasia severity at six months.<sup>24</sup> The role of the right hemisphere remains controversial and may depend upon the specific functions of given structures.

Fiber tractography, as one of the white matter segmentation methods, is not feasible in some stroke survivors, especially with large lesions. The absence of the tract with this method might provide qualitative information that can be used in prediction, as Kim and colleagues showed that the inability of manual reconstruction of the left AF predicted poor global language outcomes.<sup>23</sup> However, we used an atlas-based segmentation to obtain quantitative metrics of the tracts across all the subjects independent of the lesion site. Different groups including ours utilized this method, and it was proven to be feasible in post-stroke studies in which DTI data from patients with large lobar stroke lesions were analyzed.<sup>8,10,11</sup>

Lesion mapping provides valuable information as lesion load in the left superior longitudinal fasciculus, and arcuate fasciculus in acute aphasia predicted recovery in naming performance.<sup>43</sup> We accounted for lesion load in our analyses and utilized integrity thresholding in white matter segmentation (FA of 0.15) that eliminated the significantly injured tissues. We did not mask out the lesions automatically or mapped the lesions within the tracts, as one can speculate some of the white matter lesions seen in conventional imaging do not reflect complete disconnection. Also, lesion centric approaches have their limitations as it does not capture the downstream effects of the lesions in the big networks controlling cognitive functions.<sup>7</sup>

Several previous studies utilized multimodal imaging models, combining functional and structural connectivity,<sup>39,50</sup> in a cross-sectional manner, and concluded that multimodal imaging is superior to the unimodal imaging. Thus, one limitation of our study is that it lacks functional mapping. However, it is equally important to balance the amount of time spent in the scanner and cost with the information obtained in clinical cohorts. We believe that our findings support that DTI alone can provide valuable and clinically useful information in predicting language performance in post-stroke aphasia. Despite our efforts to reduce type I errors with recursive feature reduction model and correction for multiple comparisons, our study is also limited by a small sample size, missing time points (see figure 2 for all the data points), and only one experienced rater of the imaging data. Larger clinical studies with more time points and multiple independent raters are needed to confirm our findings.

Kurtosis-based diffusion imaging, an advanced diffusion-based technique, was also used to track therapy-related effects in language pathways and showing that the increased integrity of the left ILF predicted semantic accuracy in post-stroke aphasia,<sup>45</sup> similar to our findings.

The additional contribution of other advanced diffusion imaging techniques like diffusion spectrum imaging or intravoxel incoherent motion imaging in aphasia recovery remains to be seen.

Despite its limitations, our study confirms the importance of the microstructural integrity of left AF and ILF in measures of narrative speech over the first year after left hemisphere stroke.

## Funding Source

This work was made possible by the National Institutes of Health (National Institute of Deafness and Communication Disorders) through awards R01 DC05375 (PI: Hillis), R01 DC015466 (PI: Hillis), and P50 DC011739 (PI: Fridriksson). We gratefully acknowledge this support.

## References

1. Pedersen PM, Jorgensen HS, Nakayama H, Raaschou HO, Olsen TS. Aphasia in acute stroke: incidence, determinants, and recovery. *Ann Neurol*. 1995;38:659–666. [PubMed: 7574464]
2. Flowers HL, Skoretz SA, Silver FL, et al. Poststroke Aphasia Frequency, Recovery, and Outcomes: A Systematic Review and Meta-Analysis. *Arch Phys Med Rehabil*. 2016;97:2188–2201. [PubMed: 27063364]
3. Hillis AE. The handbook of adult language disorders, 2<sup>nd</sup> ed. New York: Psychology Press; 2013. pp204–226
4. Binder JR, Frost JA, Hammeke TA, Cox RW, Rao SM, Prieto T. Human brain language areas identified by functional magnetic resonance imaging. *J Neurosci*. 1997;17(1):353–362. [PubMed: 8987760]
5. Petersen S, Fox P, Posner M, Raichle ME. Positron emission tomographic studies of the cortical anatomy of single-word processing. *Nature*. 1988;331:585–589. [PubMed: 3277066]
6. Kertesz A, McCabe P. Recovery patterns and prognosis in aphasia. *Brain*. 1977;100:1–18. [PubMed: 861709]
7. Price CJ, Hope TM, Seghier ML. Ten problems and solutions when predicting individual outcome from lesion site after stroke. *Neuroimage*. 2017;145:200–208. [PubMed: 27502048]
8. Keser Z, Sebastian R, Hasan KM, Hillis AE. Right Hemispheric Homologous Language Pathways Negatively Predicts Poststroke Naming Recovery. *Stroke*. 2020;51:1002–1005. [PubMed: 31884909]
9. Keser Z, Kamali A, Younes K, Schulz PE, Nelson FM, Hasan KM. Yakovlev's Basolateral Limbic Circuit in Multiple Sclerosis Related Cognitive Impairment. *J Neuroimaging*. 2018;28(6):596–600. [PubMed: 29893064]
10. Marchina S, Zhu LL, Norton A, Zipse L, Wan CY, Schlaug G. Impairment of speech production predicted by lesion load of the left arcuate fasciculus. *Stroke*. 2011;42(8):2251–2256. [PubMed: 21719773]
11. Wang J, Marchina S, Norton AC, Wan CY, Schlaug G. Predicting speech fluency and naming abilities in aphasic patients. *Front Hum Neurosci*. 2013;7:831. [PubMed: 24339811]
12. Geva S, Correia MM, Warburton EA. Contributions of bilateral white matter to chronic aphasia symptoms as assessed by diffusion tensor MRI. *Brain Lang*. 2015;150:117–128. [PubMed: 26401977]
13. Ivanova MV, Isaev DY, Dragoy OV, et al. Diffusion-tensor imaging of major white matter tracts and their role in language processing in aphasia. *Cortex*. 2016;85:165–181. [PubMed: 27289586]
14. Meier EL, Johnson JP, Pan Y, Kiran S. The utility of lesion classification in predicting language and treatment outcomes in chronic stroke-induced aphasia. *Brain Imaging Behav*. 2019;13:1510–1525. [PubMed: 31093842]



15. Rosso C, Vargas P, Valabregue R, et al. Aphasia severity in chronic stroke patients: a combined disconnection in the dorsal and ventral language pathways. *Neurorehabil Neural Repair*. 2015;29:287–295. [PubMed: 25096274]
16. Jang SH. Diffusion tensor imaging studies on arcuate fasciculus in stroke patients: a review. *Front Hum Neurosci*. 2013;7:749. [PubMed: 24198780]
17. Breier JI, Juranek J, Papanicolaou AC. Changes in maps of language function and the integrity of the arcuate fasciculus after therapy for chronic aphasia. *Neurocase*. 2011;17(6):506–517. [PubMed: 22111962]
18. Schlaug G, Marchina S, Norton A. Evidence for plasticity in white-matter tracts of patients with chronic Broca's aphasia undergoing intense intonation-based speech therapy. *Ann N Y Acad Sci*. 2009;1169:385–94. [PubMed: 19673813]
19. van Hees S, McMahon K, Angwin A, de Zubizaray G, Read S, Copland DA. Changes in white matter connectivity following therapy for anomia post stroke. *Neurorehabil Neural Repair*. 2014;28:325–334. [PubMed: 24297762]
20. Wan CY, Zheng X, Marchina S, Norton A, Schlaug G. Intensive therapy induces contralateral white matter changes in chronic stroke patients with Broca's aphasia. *Brain Lang*. 2014;136:1–7. [PubMed: 25041868]
21. Bonilha L, Gleichgerrcht E, Nesland T, Rorden C, Fridriksson J. Success of Anomia Treatment in Aphasia Is Associated With Preserved Architecture of Global and Left Temporal Lobe Structural Networks. *Neurorehabil Neural Repair*. 2016;30:266–279. [PubMed: 26150147]
22. Hosomi A, Nagakane Y, Yamada K, et al. Assessment of arcuate fasciculus with diffusion-tensor tractography may predict the prognosis of aphasia in patients with left middle cerebral artery infarcts. *Neuroradiology*. 2009;51:549–555. [PubMed: 19434402]
23. Kim SH, Jang SH. Prediction of aphasia outcome using diffusion tensor tractography for arcuate fasciculus in stroke. *AJNR*. 2013;34:785–79010. [PubMed: 23042924]
24. Forkel SJ, Thiebaut de Schotten M, Dell'Acqua F, et al. Anatomical predictors of aphasia recovery: a tractography study of bilateral perisylvian language networks. *Brain*. 2014;137:2027–2039. [PubMed: 24951631]
25. Goodglass H, Kaplan E, Barresi B. *Boston Diagnostic Aphasia Examination, 3<sup>rd</sup> ed (BDAE-3)* San Antonio: Pearson; 2000.
26. Yorkston KM, Beukelman DR. An analysis of connected speech samples of aphasic and normal speakers. *J Speech Hear Disord*. 1980;45(1):27–36. [PubMed: 7354627]
27. Nicholas LE, Brookshire RH. A system for quantifying the informativeness and efficiency of the connected speech of adults with aphasia. *J Speech Hear Res*. 1993;36:338–350. [PubMed: 8487525]
28. Agis D, Goggins MB, Oishi K, Davis C, Wright A, Hillis AE. Picturing the size and site of stroke with an expanded National Institutes of Health Stroke Scale. *Stroke*. 2016;47:1459–1465. [PubMed: 27217502]
29. Stockbridge MD, Berube S, Goldberg E, Suarez A, Mace R, Ubellacker D, Hillis AE. Differences in linguistic cohesion within the first year following right-and left-hemisphere lesions. *Aphasiology*. 2019 Epub Nov 23.
30. Keator LM, Faria A, Kim T, et al. Cookie Theft Picture Description: Linguistic and Neural Correlates. Presented at the Academy of Aphasia 56th Annual Meeting; 10 21–23, 2018; Quebec, Canada. doi: 10.3389/conf.fnhum.2018.228.00097
31. Liles BZ, Coelho CA. Cohesion analysis. In: Cherney LR, Shadden BB, Coelho CA, editors. *Analyzing discourse in communicatively impaired adults*. Gaithersburg, MA: Aspen; 1998. pp. 65–84.
32. Halliday M, Hasan R. *Cohesion in English*. London, UK: Longman Group; 1976.
33. Schilling KG, Yeh FC, Nath V, et al. A fiber coherence index for quality control of B-table orientation in diffusion MRI scans. *Magn Reson Imaging*. 2019;58:82–89. [PubMed: 30682379]
34. Jiang H, van Zijl PC, Kim J, Pearlson GD, Mori S. DtiStudio: resource program for diffusion tensor computation and fiber bundle tracking. *Comput Methods Programs Biomed*. 2006;81:106–116. [PubMed: 16413083]

35. Catani M, de Schotten MT. Atlas of human brain connections. Oxford University Press; 2012. pp.239–347
36. Guyon I, Weston J, Barnhill S, and Vapnik V. Gene Selection for Cancer Classification Using Support Vector Machines. *Machine Learning*. 2002;46:389–422.
37. Mwangi B, Wu MJ, Cao B, et al. Individualized Prediction and Clinical Staging of Bipolar Disorders using Neuroanatomical Biomarkers. *Biol Psychiatry Cogn Neurosci Neuroimaging*. 2016;1:186–194. [PubMed: 27047994]
38. Yang M, Li Y, Li J, Yao D, Liao W, Chen H. Beyond the Arcuate Fasciculus: Damage to Ventral and Dorsal Language Pathways in Aphasia. *Brain Topogr*. 2017;30:249–256. [PubMed: 27324257]
39. Pustina D, Coslett HB, Ungar L, et al. Enhanced estimations of post-stroke aphasia severity using stacked multimodal predictions. *Hum Brain Mapp*. 2017;38:5603–5615. doi:10.1002/hbm.23752 [PubMed: 28782862]
40. Binder JR, Desai RH, Graves WW, Conant LL. Where is the semantic system? A critical review and meta-analysis of 120 functional neuroimaging studies. *Cereb Cortex*. 2009;19:2767–2796. [PubMed: 19329570]
41. Seghier ML. The angular gyrus: multiple functions and multiple subdivisions. *Neuroscientist*. 2013;19:43–61. [PubMed: 22547530]
42. Badre D, Wagner AD. Left ventrolateral prefrontal cortex and the cognitive control of memory. *Neuropsychologia*. 2007;45:2883–2901. [PubMed: 17675110]
43. Hillis AE, Beh YY, Sebastian R, et al. Predicting recovery in acute poststroke aphasia. *Ann Neurol*. 2018;83(3):612–622. [PubMed: 29451321]
44. Ding J, Martin RC, Hamilton AC, Schnur TT. Dissociation between frontal and temporal-parietal contributions to connected speech in acute stroke. *Brain*. 2020;143:862–876. [PubMed: 32155246]
45. McKinnon ET, Fridriksson J, Glenn GR, et al. Structural plasticity of the ventral stream and aphasia recovery. *Ann Neurol*. 2017;82:147–151. [PubMed: 28628946]
46. Harvey DY, Schnur TT. Distinct loci of lexical and semantic access deficits in aphasia: Evidence from voxel-based lesion-symptom mapping and diffusion tensor imaging. *Cortex*. 2015;67:37–58. [PubMed: 25880795]
47. Tagamets MA, Cortes CR, Griego JA, Elvevåg B. Neural correlates of the relationship between discourse coherence and sensory monitoring in schizophrenia. *Cortex*. 2014;55:77–87. [PubMed: 23969195]
48. Caplan D, Waters G, Kennedy D, et al. A study of syntactic processing in aphasia II: neurological aspects. *Brain Lang*. 2007;101:151–177. [PubMed: 16997366]
49. Pani E, Zheng X, Wang J, Norton A, Schlaug G. Right hemisphere structures predict poststroke speech fluency. *Neurology*. 2016;86:1574–1581. [PubMed: 27029627]
50. Meier EL, Johnson JP, Pan Y, Kiran S. A lesion and connectivity-based hierarchical model of chronic aphasia recovery dissociates patients and healthy controls. *NeuroImage Clin*. 2019;23:101919 [PubMed: 31491828]

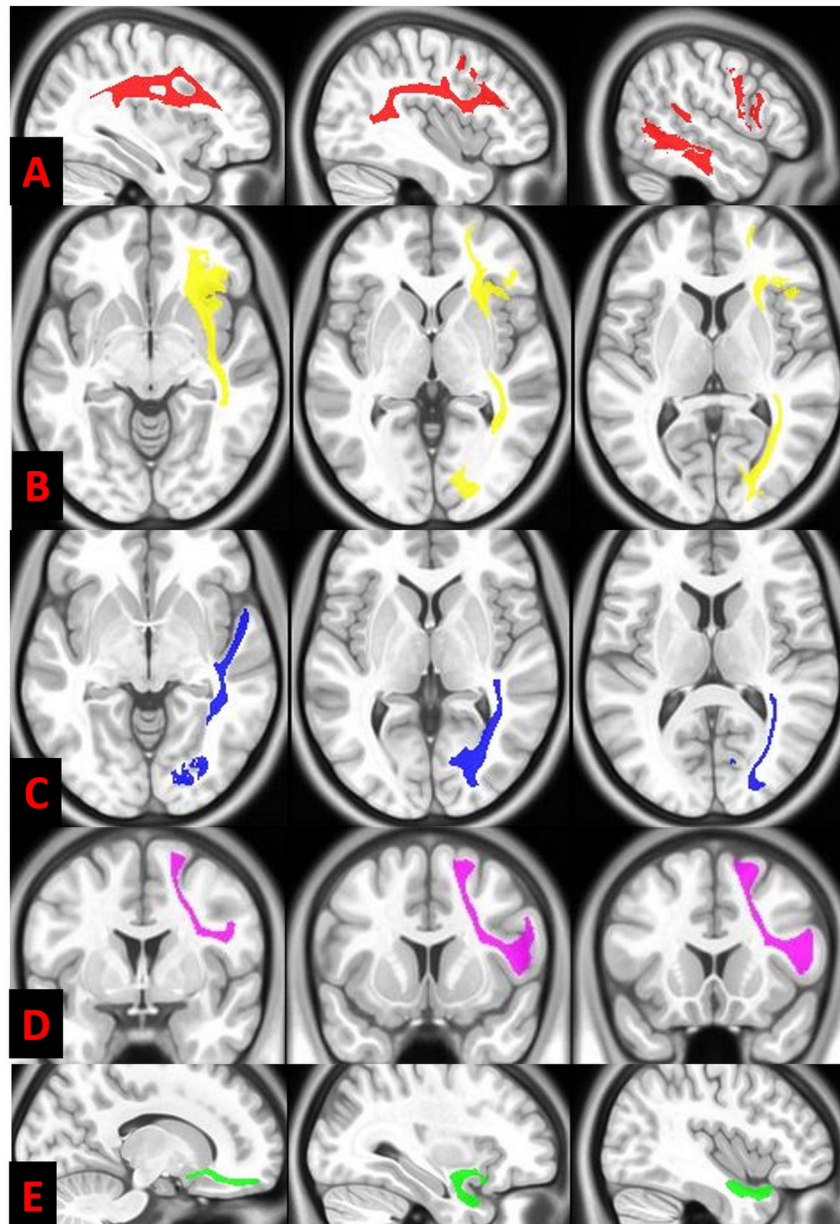


**Figure 1.** Diffusion tensor imaging white matter parcellation of the left arcuate fasciculus (in red) (A) and inferior frontal occipital fasciculus (in yellow) (B), inferior longitudinal fasciculus (in blue) (C), frontal aslant pathway (in violet) (D) and uncinate fasciculus (in green) (E) is illustrated on serial axial, coronal and sagittal T1 weighted background.



**Figure 2.** Scatter plots of all the data points (a: acute/subacute (colored in red), b: early chronic (colored in green), c: late chronic (colored in blue) from each subject (named numerically and combined with time point; e.g. “1c” represents late chronic time point from subject 1) for correct content (CU), fractional anisotropy (FA) of the left arcuate fasciculus, and the inferior longitudinal fasciculus are highlighted. Y-axis represents content units (CUs) in figure A, FA values for figures B and C. Data labels correspond to the data points in the Y-axis. Although there are no validated cut-off values to classify post-stroke aphasia under mild, moderate, or severe categories, higher CUs represent better outcomes. There was no consistent trend of increase or decrease in behavioral or imaging metrics across the time points for the patients who have more than one data point.

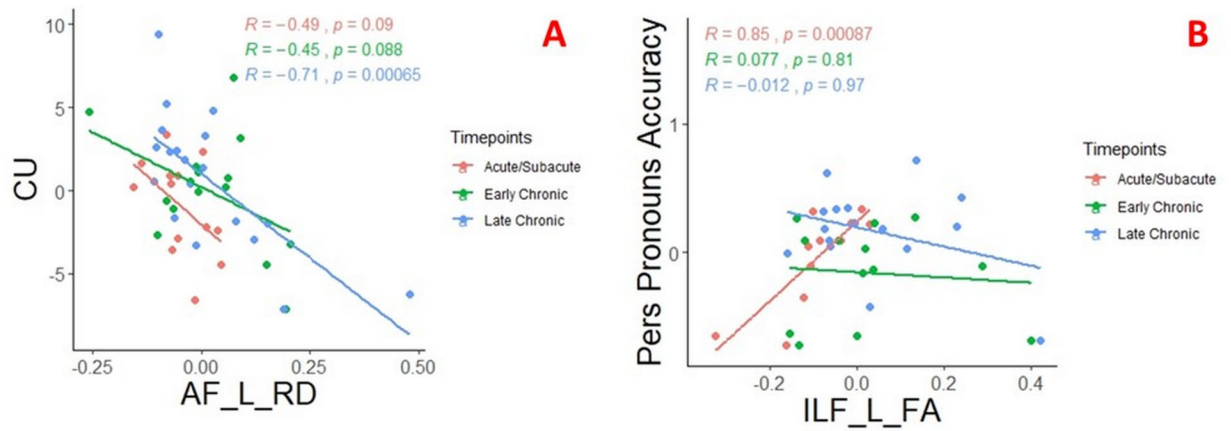


**Figure 3.**

Scatter plots, which are colored into acute/subacute, early chronic and late chronic time windows, illustrates the significant correlation between radial diffusivity of the left arcuate fasciculus (AF\_L\_RD) and the number of correct content units (CU) (A); fractional anisotropy of left inferior longitudinal fasciculus (ILF\_L\_FA) and personal pronouns accuracy (B). Of note, residuals from linear (A) and logistic regression (B) plotted to account for age, education, and lesion load in the model. Rho ( $r$ ) and p-values ( $p$ ) from partial correlation analyses are shown on the graph.

**Table 1.**

The summary of the demographics.

| Sub | Gen | Hand | Age | LL   | Edu | BNT | Lesion Location                       |
|-----|-----|------|-----|------|-----|-----|---------------------------------------|
| 1   | F   | R    | 36  | 0.08 | 14  | 30  | Left anterior CR and putamen          |
| 2   | M   | R    | 46  | 0.76 | 12  | 26  | Left Thalamus                         |
| 3   | F   | R    | 50  | 0.10 | 12  | 20  | Left anterior CR                      |
| 4   | F   | R    | 65  | 0.14 | 14  | 29  | Left meFG                             |
| 5   | M   | R    | 37  | 6.27 | 12  | 0   | Left IFG, MFG, STG, IPG               |
| 6   | F   | R    | 64  | 0.21 | 18  | 28  | Left IFG                              |
| 7   | F   | L    | 60  | 4.65 | 14  | 27  | Left IFG and anterior CR              |
| 8   | F   | R    | 41  | 0.64 | 12  | 23  | Left ALIC and extreme capsule         |
| 9   | F   | R    | 81  | 1.83 | 11  | 21  | Left posterior CR                     |
| 10  | F   | R    | 60  | 0.67 | 14  | 23  | Left IFG                              |
| 11  | M   | R    | 60  | 0.67 | 14  | 11  | Left STG and IPG                      |
| 12  | F   | R    | 56  | 0.07 | 14  | 21  | Left posterior hippocampus and cuneus |
| 13  | F   | R    | 60  | 0.50 | 14  | 27  | Left CR                               |
| 14  | M   | R    | 56  | 3.67 | 16  | 28  | Left cuneus                           |
| 15  | M   | R    | 68  | 1.71 | 18  | 27  | Left caudate nucleus                  |
| 16  | F   | R    | 36  | 1.77 | 12  | 18  | Left STG and MTG                      |
| 17  | F   | R    | 60  | 0.94 | 14  | 21  | Left IFG                              |
| 18  | F   | R    | 54  | 0.93 | 18  | 15  | Left splenium of corpus callosum      |
| 19  | M   | R    | 52  | 0.01 | 18  | 28  | Left anterior CR                      |
| 20  | F   | R    | 55  | 8.63 | 16  | 0   | Left STG and IPG                      |
| 21  | M   | R    | 65  | 0.91 | 14  | 29  | Left posterior CR                     |
| 22  | M   | R    | 60  | 0.06 | 16  | 27  | Left IFG                              |
| 23  | F   | L    | 56  | 0.42 | 18  | 27  | Left thalamic                         |
| 24  | F   | R    | 41  | 0.77 | 18  | 29  | Left anterior CR                      |
| 25  | M   | R    | 47  | 0.03 | 15  | 28  | Left superior CR                      |
| 26  | F   | R    | 61  | 0.50 | 9   | 16  | Left meFG, CG, STG                    |
| 27  | M   | R    | 60  | 0.12 | 12  | 22  | Left caudate nucleus                  |
| 28  | M   | R    | 60  | 0.09 | 16  | 29  | Left thalamic                         |

Abbreviations: ALIC: Anterior limb of internal capsule, BNT: Shorter version of Boston Naming Test (0–30), CG: Cingulate gyrus, CR: Corona radiata, Edu: Education in years, Gen: Gender, Hand: Handedness, IFG: Inferior frontal gyrus, IPG: Inferior parietal gyrus, LL: Lesion load (Stroke lesion + white matter lesions percentage to intracranial volume), MeFG: Medial frontal gyrus, MFG: Middle frontal gyrus, MTG: Middle temporal gyrus, STG: Superior temporal gyrus, Sub: Subject numbers.



**Table 2.**

For three different time points as well as the longitudinal (acute DTI metrics predicting early or late chronic behavioral scores) analyses, the p-values from the regression analyses and the rho values from the partial correlation analyses (residual values obtained the multivariable linear and logistic models) are highlighted. For statistically significant associations, the area under the curve (AUC) values from the receiver operating characteristic (ROC) for the regression models and odds ratio (OR) (with 95% confidence interval in brackets) calculations for the logistic regression models are shown. Correlations that remained significant after false discovery rate analysis is presented in bold font.

| Tract DTI Metrics               | CU           |                |             | Personal Pronouns Cohesiveness |                |          |                         |
|---------------------------------|--------------|----------------|-------------|--------------------------------|----------------|----------|-------------------------|
|                                 | Rho-value    | p-value        | AUC         | Rho-value                      | p-value        | AUC      | OR                      |
| <b>Acute/Subacute Timepoint</b> |              |                |             |                                |                |          |                         |
| Left_AF_FA                      | 0.44         | 0.76           |             | 0.66                           | 0.028          | 1        | 1.16 [1.07–1.26]        |
| Left_AF_RD                      | -0.49        | 0.09           |             | -0.22                          | 0.29           |          |                         |
| Left_IFOF_FA                    | 0.44         | 0.20           |             | 0.28                           | 0.16           |          |                         |
| Left_IFOF_RD                    | -0.65        | 0.07           |             | -0.05                          | 0.11           |          |                         |
| Left_ILF_FA                     | 0.23         | 0.59           |             | <b>0.85</b>                    | <b>0.00087</b> | <b>1</b> | <b>1.06 [1.03–1.10]</b> |
| Left_ILF_RD                     | -0.11        | 0.53           |             | -0.44                          | 0.12           |          |                         |
| <b>Early Chronic Timepoint</b>  |              |                |             |                                |                |          |                         |
| Left_AF_FA                      | 0.45         | 0.01           | 0.96        | 0.22                           | 0.16           |          |                         |
| Left_AF_RD                      | -0.45        | 0.09           | 0.97        | -0.25                          | 0.35           |          |                         |
| Left_IFOF_FA                    | 0.39         | 0.10           |             | 0.10                           | 0.22           |          |                         |
| Left_IFOF_RD                    | -0.35        | 0.13           |             | -0.02                          | 0.83           |          |                         |
| Left_ILF_FA                     | 0.41         | 0.19           |             | 0.07                           | 0.81           |          |                         |
| Left_ILF_RD                     | -0.47        | 0.01           | 0.96        | -0.04                          | 0.98           |          |                         |
| <b>Late Chronic Timepoint</b>   |              |                |             |                                |                |          |                         |
| Left_AF_FA                      | 0.60         | 0.005          | 0.86        | 0.57                           | 0.02           | 1        | 1.09 [1.03–1.14]        |
| Left_AF_RD                      | <b>-0.71</b> | <b>0.00065</b> | <b>0.87</b> | -0.59                          | 0.007          | 1        | 1.11 [1.06–1.15]        |
| Left_IFOF_FA                    | 0.49         | 0.01           | 0.86        | 0.25                           | 0.25           |          |                         |
| Left_IFOF_RD                    | -0.57        | 0.004          | 0.86        | -0.07                          | 0.23           |          |                         |
| Left_ILF_FA                     | 0.43         | 0.02           | 0.86        | -0.12                          | 0.97           |          |                         |
| Left_ILF_RD                     | -0.60        | 0.003          | 0.89        | -0.04                          | 0.19           |          |                         |
| <b>Longitudinal</b>             |              |                |             |                                |                |          |                         |
| Left_AF_FA                      | 0.01         | 0.93           |             | 0.31                           | 0.51           |          |                         |
| Left_AF_RD                      | -0.64        | 0.025          | 0.93        | -0.15                          | 0.29           |          |                         |
| Left_IFOF_FA                    | 0.08         | 0.54           |             | 0.22                           | 0.56           |          |                         |
| Left_IFOF_RD                    | -0.13        | 0.92           |             | -0.02                          | 0.21           |          |                         |
| Left_ILF_FA                     | 0.41         | 0.85           |             | 0.33                           | 0.20           |          |                         |
| Left_ILF_RD                     | -0.19        | 0.10           |             | -0.01                          | 0.93           |          |                         |

Abbreviations: AF: Arcuate Fasciculus, DTI: Diffusion Tensor Imaging, FA: Fractional Anisotropy, IFOF: Inferior Fronto-Occipital Fasciculus, ILF: Inferior Longitudinal Fasciculus, RD: Radial Diffusivity.